Int. J. Electrochem. Sci., 12 **(2017)** 6180 – 6189, doi: 10.20964/2017.07.39

International Journal of
ELECTROCHEMICAL
SCIENCE
www.electrochemsci.org

Short Communication

Electrodeposition of A Novel Pd-Ni-W Ternary Alloy Film on SS316L

Zhiheng Zhang[1], *Junlei Tang*[1,*], *Yingying Wang*[1], *Mihai Apreutesei*[2], *Hu Wang*[3]

[1] School of Chemistry and Chemical Engineering, Southwest Petroleum University, Chengdu 610500, China
[2] Université de Lyon, Institut des Nanotechnologies de Lyon INL-UMR5270, CNRS, Ecole Centrale de Lyon, Ecully F-69134, France
[3] School of Material Science and Engineering, Southwest Petroleum University, Chengdu 610500, China
[*]E-mail: tangjunlei@126.com

Received: 26 February 2017 / *Accepted:* 19 April 2017 / *Published:* 12 June 2017

Pd-Ni-W ternary alloy films were electrodeposited on 316L stainless steel. Electrolytes containing different contents (5-40 g/L) of $Na_2WO_4^{2-}$ were used. Effects of concentration of tungsten on film structure, morphology, composition, micro-hardness and corrosion resistance were studied. The addition of tungsten refined crystalline grain and promoted hardness effectively. Electrochemical results showed that with proper tungsten in electrolytic bath, obtained film had reinforced corrosion resistance in hot sulphuric acid solution.

Keywords: Electrodeposition, Pd-Ni-W film, Corrosion

1. INTRODUCTION

Stainless steel is commonly used in various applications since it was invented, due to its favourable corrosion resistance, mechanical properties. However, in some industry, stainless steel is prone to be corroded in hot non-oxidizing acid solution, and proton exchange membrane fuel cell (PEMFC) is a typical one [1], which is usually working in dilute sulphuric acid solution at 70-80°C. Because passivation of stainless steel is not stable and corrosion resistance would decrease in this media. Electrodeposition is a convenient technique can be employed to modify surface of stainless steel to obtain more ideal properties. Various Palladium (Pd) based films have been prepared on stainless steel to enhance its corrosion resistance in hot dilute sulphuric acid solution [2-4]. On the other hand, some researches have proved tungsten (W) modified stainless steel exhibit good corrosion resistance in environment of PEMFC [5,6]. In addition, the pH-potential (or Pourbaix) diagram also reveals that tungsten may exists as insoluble WO_3 in the passive film in strong acidic solution [7]. Here, we want to develop a new alloy film containing Pd and W through electrodeposition method, enhancing corrosion resistance of stainless steel in hot sulphuric acid solution. However, in general, it is known W based alloys can only be obtained through an induced codeposition from aqueous solutions with an iron group metal (i.e. Fe, Co, Ni.) [8]. Among these metals, Ni is considered to be the best choice for codeposition owing to its good corrosion resistance in aqueous media [9]. What is more, with the presence of Ni in the alloy, formability of alloy can be improved as well. Hence, ternary alloy film Pd-Ni-W is the target for investigation and the influence from various contents of WO_4^{2-} in electrolyte is studied in this paper, which has never been reported in elsewhere to the best of our knowledge.

2. EXPERIMENTAL

2.1. Elaboration for Pd-Ni-W ternary alloy film

Pd-Ni-W ternary alloy films were prepared by electrodeposition technique. 316L stainless steel (SS316L) sheets with the size of 40 mm×13 mm×2 mm were used as substrates. The composition of SS316L used in this investigation is list as following: 0.6% Si, 0.8% Mn, 0.013% P, 2.28% Mo, 17.14% Cr, 12.58% Ni, 0.014% C, 0.0073% S and Bal.% Fe, in weight percentage. Firstly, SS316L sheets were ground from 180 to 1000 grit successively on SiC abrasive paper, and then degreased in a basic solution (NaOH: 50 g/L, Na_3PO_4: 40 g/L, Na_2CO_3: 40 g/L, OP-10: 5 mL/L) at 70 °C for 10 min to remove oil and grease. This step is followed by acidic activating in 20 wt.% H_2SO_4 + 80 g/L $(NH_4)_2SO_4$ solution (pH=1) under direct current of 10 A/dm^2 during 300 s to obtain fresh surface of substrates. Finally, the activated sample is rinsed with deionized water before electrodeposition. In particular, two bulks of graphite (10 mm×15 mm×0.5 mm) were used as double anodes in electrodeposition experiment.

Table 1. Electrolytic bath composition for Pd-Ni-W and Pd-Ni films

Chemicals	Pd-Ni-W Amount (g/L)	Pd-Ni Amount (g/L)
$PdCl_2$	3.6	3.6
$NiSO_4$	21	21
NH_4Cl	60	60
$Na_3C_6H_5O_7$	21-50	21
Na_2WO_4	5-40	-
$NH_3 \cdot H_2O$ (28%)	40 mL/L	40 mL/L

Two bulks of graphite was linked with copper wire and distance of them was approximately 6 cm. The Pd-Ni films are prepared for comparison study as well. The electrolyte composition and deposition conditions of Pd-Ni-W and Pd-Ni films are presented in Table 1 and Table 2 respectively. Various contents of Na_2WO_4 were used to probe the role of WO_4^{2-} in electrodeposition, namely 5 g/L, 10 g/L, 20 g/L, 30 g/L and 40 g/L respectively (weight percentage of Na_2WO_4). Sodium from Na_2WO_4 has no influence in the system because it doesn't participate in the electrochemical process of electrodeposition. Deposited specimens were labeled from Pd-Ni-W(5 g) to Pd-Ni-W(40 g) in the paper. The solutions were prepared using distilled water (18.25 MΩ·cm) and reagent grade chemicals.

Table 2. Elaboration parameters for Pd-Ni-W and Pd-Ni films

Parameters	Values
Current density (A/dm^2)	1
pH	8~8.5
Temperature ($^{\circ}$C)	40
Frequency (Hz)	1
Duty cycle	0.8
Deposition time (s)	300

2.2. Characterisation of Pd-Ni-W films

Morphology and chemical composition of films were analysed by Scanning Electron Microscopy (SEM) (EVO MA15, ZEISS) equipped with Energy Dispersive Spectrometry (EDS) (X-Max^N, OXFORD INSTRUMENTS). The phase structures of films were characterized with X-Ray Diffraction (XRD) (X'Pert PRO, PANalaytical) using Cu-Kα radiation (V=40 kV, I=20 mA, λ= 1.548 Å).

2.3. Electrochemical corrosion behaviour

Corrosion behaviour of Pd-Ni-W film was investigated in a typical three-electrode system through an electrochemical workstation (CHI660E, CH Instrument, Inc.). The prepared specimen was connected as the working electrode. The reference electrode and the counter electrode were a mercurous sulphate electrode (MSE, E = 613 mV vs. SHE) and a platinum foil (0.6 cm^2) respectively. All the electrochemical measurements were performed in aerated 0.5 M H_2SO_4 solutions at 70°C. The samples were sealed with silica gel and left an exposed surface area of 1 cm^2. After half-hour open circuit potential (OCP) monitoring, electrochemical impedance spectroscopy (EIS) measurement was carried out in a steady state at open circuit potential, over a frequency ranging from 100 kHz to 10 mHz with amplitude of 10 mV. Thereafter, the potentiodynamic polarisation curves tests were conducted from -100 mV (vs. E_{OCP}) to +800 mV (vs. E_{OCP}) at sweep rate of 0.5 mV/s. The exchange current extrapolated at corrosion potential from Tafel extrapolation has been chosen as the criteria of reactivity of samples. We consider this exchange current as the corrosion current density and it could represent the corrosion resistance ranking of samples.

3. RESULTS AND DISCUSSION

3.1. Microstructure

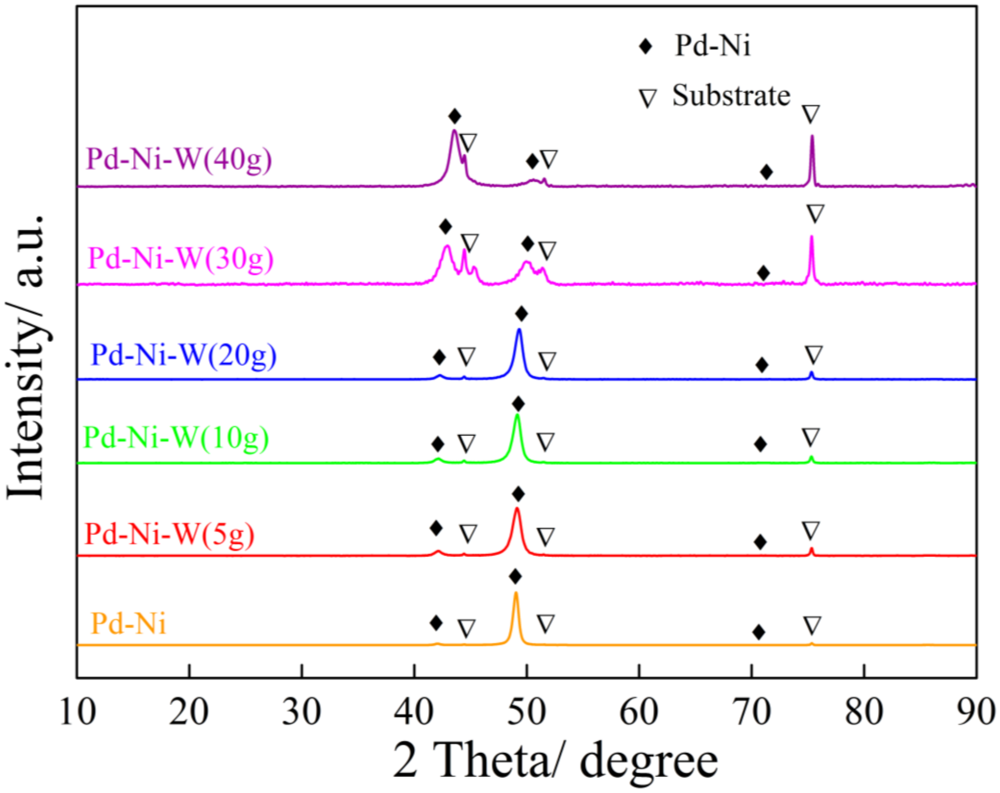

Figure 1. XRD patterns of Pd-Ni and Pd-Ni-W films deposited from aqueous solution containing various contents of WO_4^{2-}

Structural properties of Pd-Ni and Pd-Ni-W deposits are characterized by the X-ray diffraction (XRD), and results are displayed in Fig.1. All tested films exhibit a FCC crystalline phase, which indicates that substitution solid solution formed. Peaks around 2θ = 42.2 °, 49.2 °, 70.4 ° correspond to (111), (200), (220) planes of Pd-Ni solid solution phase respectively and locations of different samples shift to higher direction gradually with increase of WO_4^{2-} in electrolyte. Since the atomic mass of Ni is smaller than Pd and W, shifted peaks indicated that content of Ni in the film may increase. On the other hand, when concentration of Na_2WO_4 reaches up to 30g/L in electrolyte, the predominant plane starts to transform from the (200) plane to the (111) plane. It may be caused by the remarkably increase of tungsten atoms in Pd-Ni solid solution phase. The crystallite size of predominant plane of films is calculated according to the Scherrer's equation [10]. The results of calculated crystalline size are shown in Table 3. There is no doubt that with the presence of WO_4^{2-} in electrolyte, crystal grains sizes of alloy films are refined.

Table 3. Crystal grain sizes of predominant plane of various films

Deposits (g/L)	0	5	10	20	30	40
Grain size (nm)	17	12	12	13	11	11

3.2 Morphology and composition

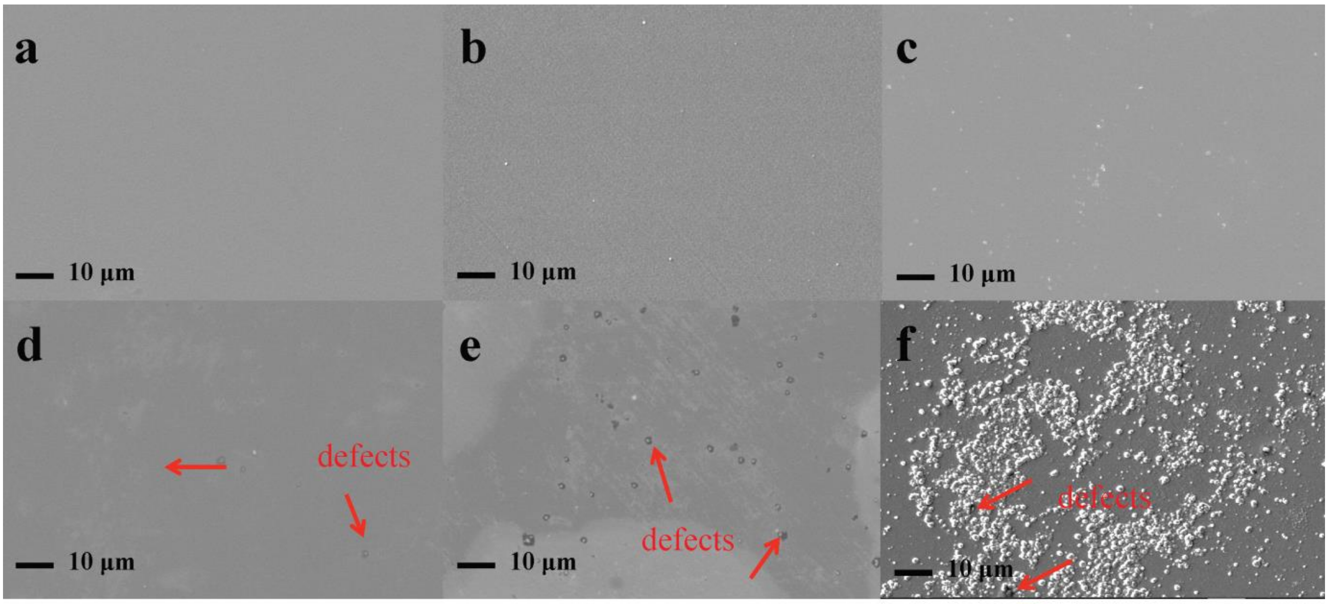

Figure 2. SEM images of Pd-Ni and Pd-Ni-W alloy films electrodeposited from aqueous solution containing different contents of Na_2WO_4 (a)0 g/L, (b)5 g/L, (c)10 g/L, (d)20 g/L, (e)30 g/L, and (f)40g/L

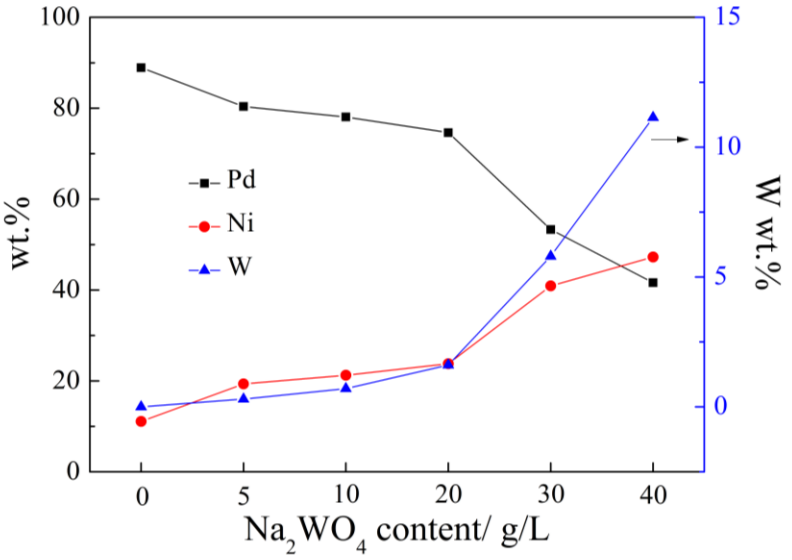

Figure 3. EDS results of Pd-Ni and Pd-Ni-W alloy films electrodeposited from aqueous solution containing different contents of WO_4^{2-}

Fig. 2 shows SEM micrographs of alloy films obtained from the electrolytic bath with different WO_4^{2-} concentrations, while the weight percentage of Pd, Ni and W of films are attached in Fig. 3. It can be seen that Pd-Ni alloy film, Pd-Ni-W alloy films deposited from electrolyte containing 5 g/L and 10 g/L Na_2WO_4 shows compact, uniform and fine surface microstructure (Fig. 2a, b and c). When the content of Na_2WO_4 in electrolytic solution is 20 g/L or higher, the obviously changes of micro-morphology can be found on the surfaces (Fig. 2d-f). From Fig. 3, the contents of Ni and W increase by increment of WO_4^{2-} in electrolyte. In contrast, the Pd content displays a downtrend tendency. The more presence of WO_4^{2-} in the bath leads to less deposited Pd in the film. This may be attributed to the catalysis effect of Pd [11]. With the catalysis of Pd, the reduction of Ni from the complex of $[(Ni)(HWO_4)(Cit)]^{2-}$ becomes much easier. On the other hand, by increasing the content of WO_4^{2-}, the content of complex $[(Ni)(HWO_4)(Cit)]^{2-}$ which is predominant in the electrolyte also will increase, since pH of the solution is around 8 [12]. Meanwhile, the deposition of Ni from its other complexes in this electrolyte occurs paralleled. Therefore, a higher content of Ni is detected in the film. Thereafter, the deposition of W is also facilitated according to Ni-W induced codeposition mechanism [8]. When a small number of WO_4^{2-} presents in electrolyte (less than 20 g/L Na_2WO_4), there is just less than 1% W presence in the film. It seems that the minute content of W in the film has little influence on micro-morphology of Pd-Ni-W film. With a further increment of WO_4^{2-} in electrolytic bath (Fig. 2d-f), some defects could be found on surface of the films. This might be caused by the hydrogen evolution reaction during the deposition process [8]. Since the hydrogen evolution is concurrent with tungsten codeposition all the time, the increasing of W deposition will bring a more dramatic hydrogen evolution. As a result, more defects are found on the surface of Pd-Ni-W film with increment of WO_4^{2-} in electrolyte (30 g/L Na_2WO_4). When the content of Na_2WO_4 in electrolyte is 40 g/L, the weight percentage of W in the film reaches up to more than 11.14%. The Pd-Ni-W alloy film deposited from electrolyte containing 40 g/L Na_2WO_4 presents an agglomerates of nodules morphology, which is very similar to the morphology of Ni-W based deposits [13,14].

3.3. Electrochemical test

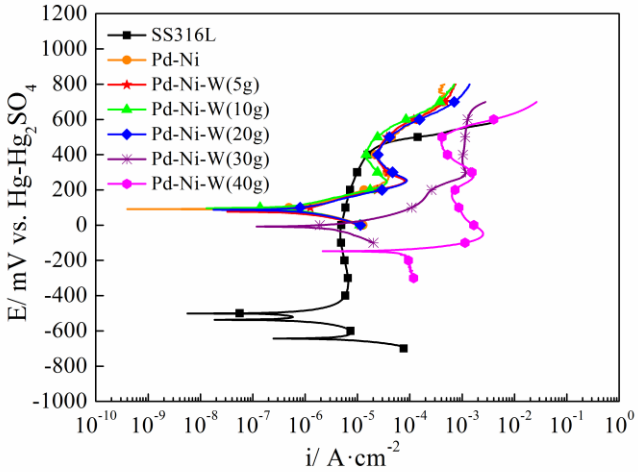

Figure 4. Potentiodynamic polarisation curves of SS316L and different deposited alloy films in 0.5 M H_2SO_4 solution at 70°C

Fig. 4 shows the polarisation curves measured on SS316L and the sample with different deposited alloy films. The corrosion potential (E_{corr}) and the corrosion current density (i_{corr}) of all specimens are determined through Tafel's extrapolation method and the corrosion resistance of films is evaluated in terms of i_{corr}. The obtained results are listed in Table 4.

Table 4. Corrosion potentials and corrosion current densities of specimens

Specimen	E_{corr}/ (mV, MSE)	i_{cror}/($\times 10^{-6}$A/cm^2)	β_c/ (mV/dec)	β_a/ (mV/dec)
SS316L	-666	24.141	13.1	-
Pd-Ni	91	1.021	72.7	76.5
Pd-Ni-W(5 g)	78	0.586	71.7	82.4
Pd-Ni-W(10 g)	102	0.842	87.3	77.7
Pd-Ni-W(20 g)	88	1.109	81.5	76.3
Pd-Ni-W(30 g)	-14	2.604	81.4	59.5
Pd-Ni-W(40 g)	-138	47.548	160.9	17.4

First of all, as for bare SS316L, the corresponding corrosion current density at corrosion potentials of -666 mV_{MSE} is quite high and active dissolution happens. Then, with potential raising (between -600 mV_{MSE} and -400 mV_{MSE}), active-passive oscillating behaviour [15] of SS316L could be found, and the stable passivation of the specimen only can be achieved above -300 mV_{MSE}. The corrosion potential shifts to positive direction when Pd-based films is deposited on stainless steel. Thus the protection mechanism of Pd-Ni-W film is not only from barrier effect but also anodic polarisation effect, which makes stainless steel substrate be in stable passivation.

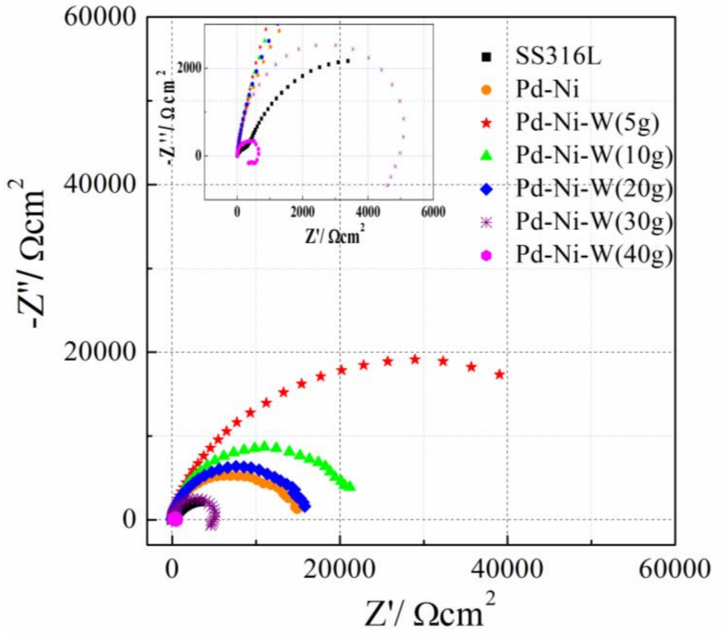

Figure 5. Nyquist plots of SS316L and deposited different alloy films in 0.5 M H_2SO_4 solution at 70°C

For the Tafel slope, the anodic Tafel slope (β_a) of SS316L was not calculated owing to the oscillation of anodic current densities in the active-passive transition zone. The corrosion of SS316L at corrosion potential is in active dissolution, so that the cathodic reaction (mainly hydrogen evolution reaction, oxygen reduction also exists because the test solution is open to air) can determine its corrosion rate. On the contrast, the cathodic reaction of alloy film protected specimens may only involve oxygen reduction because their potential are much higher. The difference in cathodic Tafel slopes (β_c) of alloy film protected specimens indicates the difference in cathodic kinetics. The β_c probably is relative to the chemical composition and the preferred lattice orientation of different alloy films. However, the corrosion rate of alloy film protected specimens is directly associated with the anodic process of metal dissolution. It can be seen the β_a of Pd-Ni film is 76.5 mv/dec, while its calculated values of the specimens deposited from electrolyte containing 5 g/L and 10 g/L Na_2WO_4 are 82.4 and 77.7 respectively. The lager value of β_a may be relative to a stronger inhibition effect on the anodic process when the film contains proper content of alloying tungsten. When the electrolyte containing more than 10 g/L Na_2WO_4, the β_a decreases with the increase of WO_4^{2-} in electrolyte. On another hand, it is seen specimens with the alloy film deposited from electrolyte containing 5 g/L and 10 g/L Na_2WO_4 have relatively smallest values of i_{corr}, indicating these samples own better corrosion resistance than others in this corrosive medium. Comparing with Pd-Ni alloy film, they have a decreased crystallite size, which is a beneficial effect in improving corrosion resistance. Then, the corrosion resistance of samples prepared from the electrolyte containing higher contents of WO_4^{2-} decreases. Based on characterisation results presented above, the deteriorated corrosion resistance may be attributed to two aspects: one is morphology, while another is related to composition of films. It is obvious that with an increment of WO_4^{2-} in electrolytic bath, the content of W in films sees a growing trend. Meanwhile, the Pd-Ni-W film possesses more defects obtained. Defective films make more substrate exposed to corrosive medium, consequently corrosion rates of samples are accelerated. On the other hand, the content of Pd in Pd-Ni-W film reduces with increasing WO_4^{2-} in electrolyte. Since the noble metal Pd plays a significant role in anodic polarisation effect, the passivation ability of SS316L substrate will decrease if the content of Pd in Pd-Ni-W film is too low.

Electrochemical impedance of Nyquist plots of samples deposited from electrolytes containing various WO_4^{2-} in sulphuric acid at high temperature is presented in Fig. 5. It is noted that the specimen deposited from electrolyte containing 5 g/L Na_2WO_4 shows the largest impedance arc in comparison with others. Compared with the Pd-Ni alloy coated specimen, the film obtained from the electrolyte containing 5 g/L Na_2WO_4 has much larger impedance arc. However, with a further addition of WO_4^{2-} into the electrolytic solution, the impedance arcs of obtained samples see a decreasing trend. Furthermore, parts of EIS spectra of two samples deposited from electrolyte containing 30 g/L and 40 g/L Na_2WO_4 are in the fourth quadrant, indicating the presence of inductive reactance. It is related to the dissolution of coatings and the generation of corrosion products [14].

3.4. Micro-hardness measurement

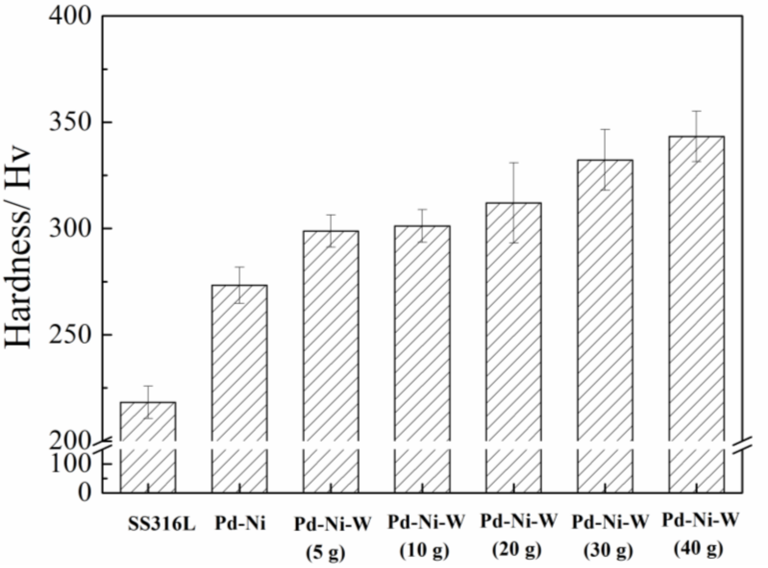

Figure 6. Micro-hardness of SS316L and deposited specimens

Fig. 6 shows the micro-hardness of bare stainless steel and alloy film coated samples. SS316L has the lowest average hardness value of ~ 218 Hv. The hardness is improved to 273 Hv when Pd-Ni alloy film was deposited. With the presence of W in the film, hardness values of deposited specimens see an upward tendency. When the content of W reached up to 11.14% in the film, hardness of the sample has the largest value ~ 343 Hv. As for strengthened hardness mechanism, it can be attributed to increased content of tungsten and grain refinement in films, which is corresponding to EDS and XRD results.

4. CONCLUSION

A noble Pd-Ni-W ternary alloy film was prepared through electrodeposition method from aqueous solution. When tungsten was presence in the film, crystallite was refined. A growing content of WO_4^{2-} is presence in electrolytic bath for electrodeposition will cause an increment of nickel and decrease of palladium in the obtained film. Proper content of tungsten in the film can have a good anti-corrosion performance for stainless steel in hot sulphuric acid solution. Furthermore, micro-hardness values of obtained specimens see an increasing trend with increment of tungsten content in the films. Consequently, electrodeposited Pd-Ni-W ternary alloy film on SS316L can improve its mechanical properties and corrosion resistance remarkably. The Pd-Ni-W alloy film coated stainless steel is a potential material for the bipolar plate in PEMFC fuel cells.

ACKNOWLEDGEMENT
This investigation is financially supported by Qihang Science Research founding of Southwest Petroleum University, Nos. 2014QHZ015, 2015QHZ013.

References

1. R. Taherian, *J. Power Sources*, 265 (2014) 370.
2. P. Ju, Y. Zuo, Y. Tang, X. Zhao, *Corros. Sci*. 66 (2013) 330.
3. L. Xu, Y. Zuo, J. Tang, Y. Tang, P. Ju, *Corros. Sci*. 53 (2011) 3788.
4. J. Tang, Y. Zuo, *Corros. Sci.* 50 (2008) 2873.
5. J. Cui, Z. Yao, F. Cheng, Y. Cui, G. Wang, L. Wang, et al., *RSC Adv*. 6 (2016) 31367.
6. L.X. Wang, J.C. Sun, S. Li, S.J. Ji, Z.S. Wen, B. Jing, *Fuel Cells*. 13 (2013) 1131.
7. M. Pourbaix, NACE, Huston, 1974. 280.
8. M.P.Q. Argañaraz, S.B. Ribotta, M.E. Folquer, L.M. Gassa, G. Benítez, M.E. Vela, et al., *Electrochim. Acta*. 56 (2011) 5898.
9. P. de Lima-Neto, A.N. Correia, R.A.C. Santana, R.P. Colares, E.B. Barros, P.N.S. Casciano, et al., *Electrochim. Acta*. 55 (2010) 2078.
10. V.M. Dalfard, *Int. J. Electrochem. Sci.* 7 (2012) 3537.
11. Y. Shacham-Diamand, A. Inberg, Y. Sverdlov, N. Croitoru, *J. Electrochem. Soc*. 147 (2000) 3345.
12. O. Younes, L. Zhu, Y. Rosenberg, E. Gileadi, *Langmuir*. 17 (2001) 8270.
13. Y. Boonyongmaneerat, K. Saengkiettiyut, S. Saenapitak, S. Sangsuk, *Surf. Coatings Technol.* 203 (2009) 3590.
14. A.L.M. Oliveira, J.D. Costa, M.B. De Sousa, J.J.N. Alves, A.R.N. Campos, R.A.C. Santana, et al., *J. Alloys Compd.* 619 (2015) 697.
15. Y. Li, M.B. Ives, K.S. Coley, *Corros. Sci.* 48 (2006) 1560.